

## 液体ヘリウム中における不純物スペクトルへの密度汎関数法の応用

## Application of density functional theory to impurity spectra in liquid helium

中務 孝 (東北大理)、矢花一浩 (筑波大物理)、George Bertsch (Univ. of Washington)

密度汎関数法 (DFT) を超流動液体ヘリウムの摂動下における原子スペクトルの解析に応用する。ヘリウムに対する原子 DFT を不純物原子まわりのヘリウムの分布を決定するのに用い、次に、電子 DFT を用いて、ヘリウム配位のアンサンブルで平均化した、原子の励起を求める。この理論で、D1 および D2 の吸収ラインのずれと幅の広がり非常にうまく説明できる。密度汎関数法が、さらに複雑な環境下でのラインシフトや幅の広がりを記述するのに有用であることを示唆する結果である。

## 1 Spectroscopy in liquid helium

Spectroscopic measurements of impurity atoms and molecules in superfluid helium have been attracting considerable interest in recent years [1, 2]. The repulsive force between an impurity and helium atoms induces a bubble around the impurity. This leads to a weak perturbation of helium atoms on the spectra of impurities. The line shifts and spectral shapes induced by the helium perturbation provide information on the properties of the bubble in the quantum liquid as well as the excited states of the impurity. Since the perturbation is weak, this method also provides a unique tool for spectroscopic measurements of atomic clusters at low temperature [2].

Because of its simplicity, perturbations on alkali-atom lines have been studied extensively [1, 3, 4]. For cesium (Cs) atoms, there are two *s*-to-*p* transitions, the  $D_1$  ( $s_{1/2} \rightarrow p_{1/2}$ ) and  $D_2$  ( $s_{1/2} \rightarrow p_{3/2}$ ) lines, both of which are blue-shifted and acquire widths in a helium bath. The shifts and widths of the two lines are different, and the  $D_2$  line has a skewed shape suggesting a double-peak structure. These features were first analyzed with a collective vibration model of the helium bubble [3, 4]. That model reproduced average peak shifts, but gave line widths less than a half of observed ones. A more sophisticated analysis has been made treating the liquid helium environment by the Path-Integral Monte-Carlo method [5]. However, the method is very costly in computer resources and is difficult to apply to more complex systems. We will show that a density functional theory (DFT) together with a statistical treatment of helium configurations provides a simple and quantitative description for the helium perturbations.

## 2 Formalism

*DFT-plus-statistical description of liquid helium*

The energy of liquid helium in the DFT is assumed to have the form,  $E = \int d\mathbf{r} \mathcal{H}_0(\mathbf{r})$ , where we adopt the Orsay-Paris functional [6],

$$\mathcal{H}_0(\mathbf{r}) = \frac{1}{2m} \left| \nabla \sqrt{\rho(\mathbf{r})} \right|^2 + \frac{1}{2} \int d\mathbf{r}' \rho(\mathbf{r}) \rho(\mathbf{r}') V_{\text{LJ}}(|\mathbf{r} - \mathbf{r}'|) + \frac{c}{2} \rho(\mathbf{r}) (\bar{\rho}_{\mathbf{r}})^{1+\gamma}. \quad (1)$$

Here,  $m$  is the mass of a helium atom and  $\bar{\rho}_{\mathbf{r}}$  is a coarse-grained density, and  $V_{\text{LJ}}$  is a screened Lennard-Jones potential.

The effect of the impurity was treated by including in Eq. (1) a potential interaction,  $V_I(\mathbf{r})$ , between the helium atoms and the impurity,

$$\mathcal{H}(\mathbf{r}) = \mathcal{H}_0(\mathbf{r}) + V_I(\mathbf{r})\rho(\mathbf{r}). \quad (2)$$

We approximate the  $V_I(\mathbf{r})$  as a contact interaction,

$$V_I(\mathbf{r}) = \frac{2\pi a}{m_e} \rho_e(\mathbf{r}), \quad (3)$$

where  $m_e$  is the electron mass and  $\rho_e(\mathbf{r})$  is the electron density of the impurity which is calculated with the electronic DFT in Sec. 2. The scattering length,  $a$ , is determined from the observed low-energy electron-helium cross section.

Utilizing the energy functional,  $E[\rho] = \int d\mathbf{r} \mathcal{H}(\mathbf{r})$ , we calculate the density profile of liquid helium, putting the impurity atom at the origin. Minimizing the grand potential at zero temperature,  $\Omega \equiv E[\rho(\mathbf{r})] - \mu N$ , leads to a Hartree-type equation

$$\left[ -\frac{1}{2m} \nabla^2 + U(\mathbf{r}) + V_I(\mathbf{r}) \right] \sqrt{\rho(\mathbf{r})} = \mu \sqrt{\rho(\mathbf{r})}. \quad (4)$$

The equation is solved with the boundary condition that the density go to the bulk density  $\rho_0$  at large  $r$ . Results indicate a sharp rise in the helium density at  $r \approx 6 \text{ \AA}$ . This corresponds to the bubble radius.

We use the  $\rho(\mathbf{r})$  computed above to generate an ensemble of configurations of helium atoms as follows. Take a large volume surrounding the alkali atom and denote it as  $V$ . This volume includes  $N$  helium atoms on average, where  $N$  is given by  $\int_V d\mathbf{r} \rho(\mathbf{r}) = N$ . We randomly sample  $N$  helium positions in  $V$  according to the density distribution  $\rho(\mathbf{r})$ . This sampling procedure gives probability distribution,  $w(\mathbf{r}_1, \dots, \mathbf{r}_N) = \prod_{i=1}^N (\rho(\mathbf{r}_i)/N)$ .

### Helium perturbation on spectra

Orbital wave functions of valence electrons in impurity,  $\psi(\mathbf{r})$ , are calculated using DFT with Dirac wave functions and kinetic energy operator. We need accurate wave functions at large distances from the atom, which cannot be achieved with the traditional LDA functional due to the incorrect orbital eigenvalues and the incorrect asymptotic behavior of the potential. As is well known, these problems are diminished with the generalized gradient approximation (GGA), which was designed to produce the correct asymptotic behavior of the potential.

We use first-order perturbation theory to evaluate the orbital shifts in the ensemble of helium configurations  $\tau = (\mathbf{r}_1, \dots, \mathbf{r}_N)$ . The same helium configuration is used for the ground state  $s_{1/2}$  and excited states  $p_{1/2}$  and  $p_{3/2}$ , following the Frank-Condon principle. For  $s_{1/2}$  and  $p_{1/2}$  states, the energy shifts of the valence electron is then calculated as  $\Delta E^{(k)}(\tau) = (2\pi a/m_e) \sum_i |\psi^{(k)}(\mathbf{r}_i)|^2$ , where  $k$  stands for orbital quantum numbers ( $lj$ ) and either  $m$  state

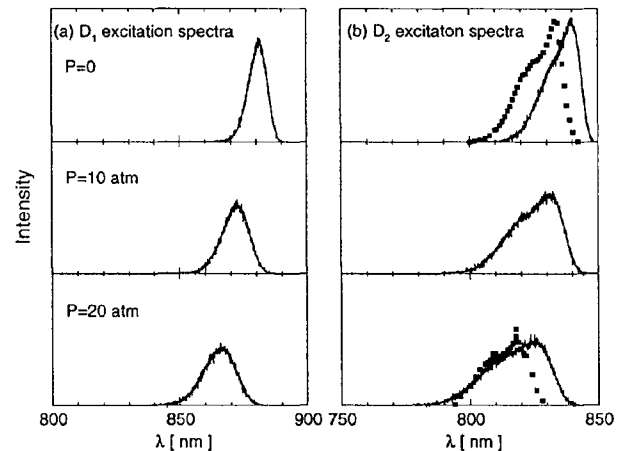


**Fig. 1** Cs  $D_1$  and  $D_2$  excitation spectrum at different helium pressure;  $P = 0, 10, \text{ and } 20 \text{ atm}$ .

may be taken. For  $p_{3/2}$  states, the matrix elements depend on  $m$  and we have to diagonalize a  $4 \times 4$  matrix to get the energy shifts. We then obtain two eigenenergies, each of which is doubly degenerate.

Each helium configuration produces an energy shift and possible splitting but the transitions remain sharp. The line broadening comes from the ensemble average over helium configurations. The line shape of the  $D_1$  ( $s_{1/2} \rightarrow p_{1/2}$ ) transition is given by

$$S_{D_1}(E) = \int_V d\tau w(\tau) \delta(E - (\Delta E^{(p_{1/2})}(\tau) - \Delta E^{(s_{1/2})}(\tau))), \quad (5)$$

where  $E$  is a shift from the energy position of the free atom. For the  $D_2$  ( $s_{1/2} \rightarrow p_{3/2}$ ) transition, we have a similar expression but need to add the two eigenmodes.

To calculate line shapes of the Cs  $D$  transitions in liquid helium, we evaluated Eq. (5) by sampling 100 000 helium configurations, generated according to the DFT density profiles. The calculated energy shifts are added to the observed  $D$  lines of free Cs atom ( $\lambda = 894.9$  nm for  $D_1$  and 852.7 nm for  $D_2$ ). Then, the intensity is estimated by counting number of events in bins of wavelength  $\Delta\lambda = 0.1$  nm. The obtained intensity spectra are shown in Fig. 1. The  $D_1$  line can be well approximated by a single Gaussian, while the  $D_2$  line has a double-peaked structure. The calculated line shifts and shapes agree with experimental observations [3, 4].

### 3 Conclusion

We have developed a simple model to describe atomic spectra of impurities embedded in the superfluid helium. Various features in the atomic spectrum of Cs, including line shifts, broadening, and skewness, are nicely reproduced in our calculation without any adjustable parameters. The model is simple enough to apply to more complex chromophores such as molecules and clusters. Detailed analysis is found in our recent paper [7].

### References

- [1] J. P. Toennies and A. F. Vilesov, *Annu. Rev. Phys. Chem.* **49**, 1 (1998).
- [2] C. Callegari *et al*, Preprint: physics/0109070 (2001).
- [3] T. Kinoshita *et al*, *Phys. Rev. A* **52**, 2707 (1995).
- [4] T. Kinoshita *et al*, *Phys. Rev. B* **54**, 6600 (1996).
- [5] S. Ogata. *J. Phys. Soc. Japan*, **68**, 2153 (1999).
- [6] J. Dupont-Roc *et al*, *J. Low Temp. Phys.* **81**, 31 (1990).
- [7] T. Nakatsukasa, K. Yabana, and G. F. Bertsch, *Phys. Rev. A*, in press; Preprint: physics/0110032.